Astron. Astrophys. 341, 211–215 (1999)

ASTRONOMY AND ASTROPHYSICS

Observational constraints on the efficiency of acceleration in the optically thin parts of Wolf-Rayet winds

S.V. Marchenko[1,2] **and A.F.J. Moffat**[1,2]

[1] Département de Physique, Université de Montréal, C.P. 6128, Succ. "Centre-Ville", Montréal, Qc, H3C 3J7, Canada
[2] Observatoire du mont Mégantic (e-mail: sergey; moffat@astro.umontreal.ca)

Received 27 March 1998 / Accepted 29 September 1998

Abstract. Wolf-Rayet stars have such strong winds that their inner regions are optically thick, preventing us from seeing the hydrostatic stellar cores. One might expect considerable acceleration of the wind to occur in the optically thick part. However, we show *empirically* that at least 50%, and in some cases up to 100%, of the wind's acceleration occurs in the optically *thin* part of the WR wind.

Key words: stars: mass-loss – stars: Wolf-Rayet

1. Introduction

The fast, dense winds of Wolf-Rayet (WR) stars are suspected to be driven primarily (if not solely) by radiation pressure. However, consistent treatment of the radiation transfer problem with strong coupling to the dynamical structure of the WR atmosphere (Schmutz 1997) can be performed only for the optically thin part of the wind. While the mechanism(s) of the initial acceleration of the wind in the optically thick, inner zone await(s) clarification (e.g. Eichler, Bar Shalom & Oreg 1995), our goal here is to impose limits on directly observable (or at least, directly deducible from observation) characteristics, thus helping to constrain the parameters required in modeling.

Subdivision of WR winds into optically thick and thin domains immediately introduces one more free parameter: a 'photospheric' wind velocity, i.e. the velocity ($v \geq 0$, by convention) at the inner boundary of the optically thin part of the expanding WR wind. This velocity, referred to as $\mathrm{v_{phot}}$, can be deduced from the weak 3-n He II emission lines in the UV region via detailed modeling (Schmutz 1997), or by measuring the velocity corresponding to the minimal intensity (maximal absorption) in the absorption troughs of P Cygni profiles (Willis 1982; Abbott & Conti 1987). Both approaches may overestimate the true value of $\mathrm{v_{phot}}$: pure *emission* lines or the *emission* parts of P Cygni profiles sample regions of the wind above the photospheric level; the velocity corresponding to the maximum absorption is above $\mathrm{v_{phot}}$ in most cases, depending on the specific line and the wind velocity gradient. As we show in this paper, we can reduce (and sometimes completely eliminate) this inevitable overestimation by assigning $\mathrm{v_{phot}}$ to the velocity in the violet-displaced P Cygni absorption where the line flux equals the continuum level as the line changes from absorption to emission (Fig. 1). In doing this, we introduce the ratio $\mathrm{v_{phot}/v_\infty}$, which in practice yields a lower limit to the efficiency of acceleration in the optically thin part of the wind. We shall try to evaluate this ratio empirically in a number of WR stars and investigate its dependence on spectral subclass.

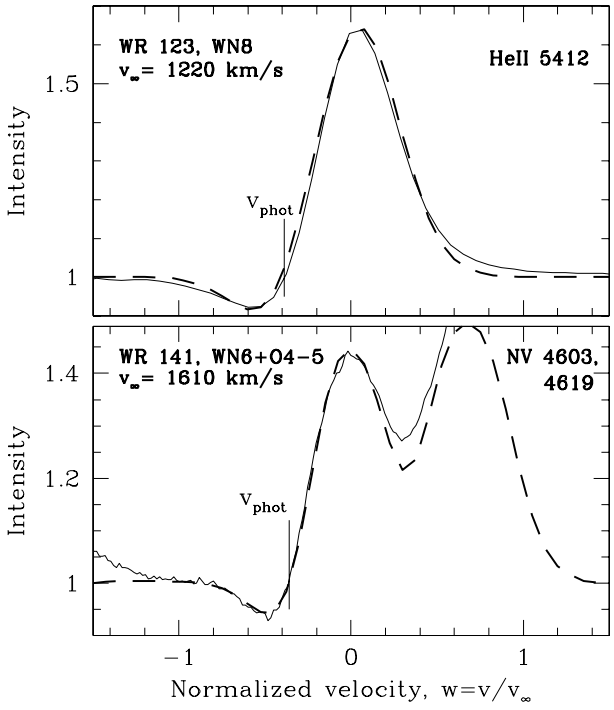

Fig. 1. Typical examples of observed (*full line*) and modeled (*dashed line*) P Cygni profiles with the estimated values of $\mathrm{v_{phot}}$ for two WR stars. Note: (1) the pronounced red wing of the observed He II 5412 line is presumably caused by electron scattering (cf. Hillier 1991; this effect is not included in the SEI model). (2) The deviations between observation and model in the red wing of the NV 4603 line are due to blending with the strong N III emission feature.

2. Available observations

We limit our measurements to WR stars of the nitrogen sequence; we thus avoid the problem of severe blending in WC

Send offprint requests to: S.V. Marchenko

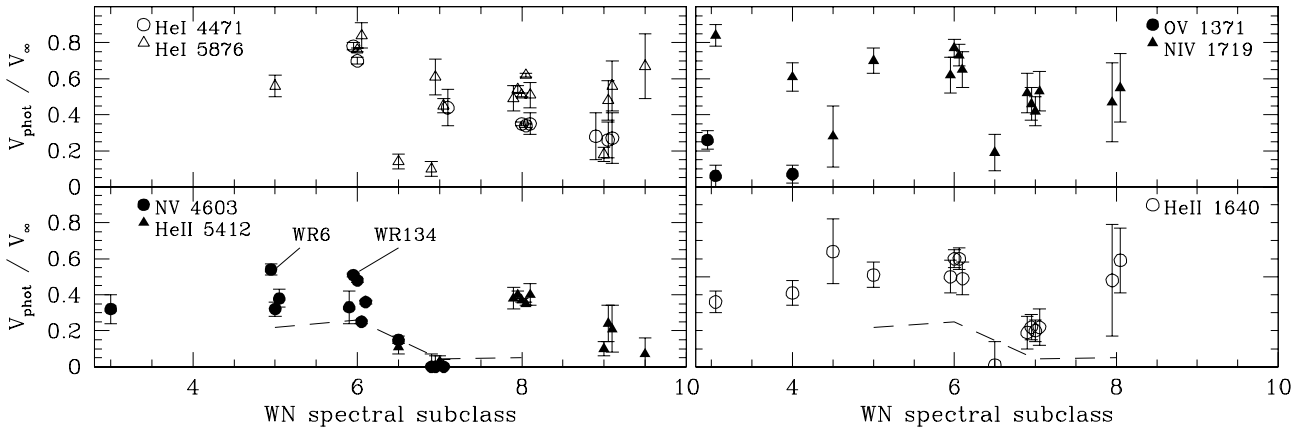

Fig. 2. Spectral dependence of the v_{phot}/v_{∞} ratio derived from optical (*left panels*) and UV lines (*right panels*). The broken line indicates the result of modeling after binning into spectral subclass. The plotted 2σ error bars account for the uncertainties in measurements of v_{phot} and v_{∞}. For clarity, some points are horizontally shifted by $\pm$(0.05-0.1).

spectra. We use all available optical and UV data: our own collection comprises very high signal-to-noise ($S/N \gg 200$), medium-resolution (0.4–1.8 Å/pixel), optical spectra of WR 6, 40, 123, 124, 134, 136, 138, 139, 141, 148, 151, 155, 156 (cf. Marchenko et al. 1998b and references therein). We also use the mean spectra from the UV atlas of St-Louis (1990), as well as the data from Moffat & Seggewiss (1978), Willis (1982), Willis & Stickland (1990), Niemela, Cabanne & Bassino (1995), and Crowther et al. (1995a–c). To measure v_{phot} in binary stars, we use the spectra taken around quadratures, thus reducing the influence of the wind-wind interaction and proximity effects (cf. Marchenko et al. 1997). Also, we allow for binary motion. If significant spectral variations occur (the best example is WR 6: St-Louis et al. 1995; Morel, St-Louis & Marchenko 1997), we take the minimal value of v_{phot}. For the estimation of v_{phot} we choose a wide variety of lines with well-developed P Cygni absorptions. We also favor transitions with the highest ionization potential, as they are presumably formed closest to the WR 'photosphere'. For a given star, the terminal velocity is derived by averaging all published estimations (Crowther et al. 1995 a-c; Rochowicz & Niedzielski 1995 and references therein). Finally, the observed values of v_{phot} and v_{∞} are corrected for radial motion of the star which, to good approximation on the average, can be obtained from the law of Galactic rotation and basic Solar motion, following Moffat et al. (1998). A relatively rare exception is the star WR 124, whose extreme runaway velocity can be deduced from its surrounding nebula.

3. Results

3.1. v_{phot}/v_{∞} *ratios measured in the optical/UV spectra*

We list in Table 1 for each star: the star name; the spectral subclass (mainly from van der Hucht et al 1988, and Crowther et al. 1995 a-c); the averaged v_{∞} along with the errors derived during the averaging (if there is only one measurement, we assume 10% accuracy); the derived minimal values of v_{phot} along with errors; and the ratio of v_{phot}/v_{∞} with $\pm\sigma$ errors taking into account the uncertainties in v_{phot} and v_{∞}.

Plotting the measured v_{phot}/v_{∞} ratio versus WN spectral subtype (Fig. 2), we note that the following lines can be used as relatively good indicators of v_{phot}: in the optical, we rely on the NV 4603 Å line, as the line with the highest ionization potential; this is replaced by the He II 5412 Å line, backed by the He I 4471 Å line in WN8-10 stars (where the NV line practically disappears, and the He I 5876 Å line leads to systematically overestimated values of v_{phot}). In the UV region the situation is much less favorable: practically all estimations, even with the best line, He II 1640 Å, lead to slightly larger values of v_{phot}, as compared to the optical (Fig. 2). This can be naturally explained as due to the strong emission component partially filling in the P Cygni absorption trough. This is quite unfortunate, because the UV should be preferred over the optical, owing to the lower optical depth of the UV continuum (Schmutz 1997). The only exception is O V 1371 Å, measurable only in the hottest WNE spectra.

Relying only on the lines that provide minimal values of v_{phot}, we immediately note the significant drop in the v_{phot}/v_{∞} ratio around WN7 spectral subclass. Also, the WN8 subclass remains apart from the neighboring WN7 and WN9-10 subclasses. These peculiarities may be the result of the following circumstances: (a) The WN7 stars probably have much steeper ionization/excitation gradients than other WN stars (Willis 1982). The steeper ionization gradient should facilitate the radiative acceleration of the wind, thus relieving the requirements of a subphotospheric velocity boost or, alternatively, substantially reducing the line optical depth at v_{phot} via a steeper velocity gradient. (b) As for the WN8 stars, the apparently high values of v_{phot}/v_{∞} may reflect the enhanced 'turbulence' of WN8 winds: this particular subgroup persistently demonstrates the highest level of activity among the whole WR population (Marchenko et al. 1998a).

Is there any dependence of v_{phot}/v_{∞} on basic stellar parameters, namely $L_{\star}$, $\dot{M}$, $R_{\star}$, $T_{\star}$? From the very beginning,

Table 1. Estimation of the v_{phot}/v_∞ ratio for WN stars

Star	Sp	v_∞	Measured		Modeled
			v_{phot}	v_{phot}/v_∞	v_{phot}/v_∞
WR 46	WN3p+c(?)	2620±270	680±100	0.26±0.05	–
WR 97	WN3+O5-7	2500±500	810±100	0.32±0.08	–
WR 152	WN3	1780±10	100±100	0.06±0.06	–
WR 128	WN4 (SB1)	1940±120	130±100	0.07±0.05	–
WR 10	WN4-5	1540±10	440±260	0.28±0.17	–
WR 6	WN5	1820±40	980±50	0.54±0.03	0.22 (0.5)[a]
WR 139	WN5+O6V-III	1800±50	570±70	0.32±0.04	0.10 (0.17)[b]
WR 151	WN5+O5V	2000[c]±200	770±70	0.38±0.05	0.12
WR 8	WC4+WN6	1650±160	540±130	0.33±0.09	–
WR 71	WN6 (SB1)	1470±30	740±130	0.50±0.09	–
WR 134	WN6+c(?)	1900±30	970±10	0.51±0.01	0.38
WR 136	WN6 (SB1)	1660±30	790±10	0.48±0.01	0.2-0.3
WR 138	WN6+OB	1420±30	350±10	0.25±0.01	0.15
WR 141	WN6+O4-5	1610±40	580±15	0.36±0.01	0.24
WR 155	WN6[7]+O9II-I	1410±70	20±260	0.01±0.13	0.04
WR 22	WN7+O6.5-8.5	1430±150	0±100	0.00±0.07	–
WR 24	WN7+a	1710±220	0±100	0.00±0.06	–
WR 25	WN7+a	1910±300	50±50	0.03±0.03	–
WR 78	WN7	1270±40	0±50	0.00±0.04	–
WR 148	WN7+B(c?)	1200±270	530±20	0.44±0.10	0.05
WR 16	WN8	830 ±50	320±50	0.38±0.06	–
WR 40	WN8	970 ±30	390±20	0.40±0.02	0.03
WR 123	WN8 (SB1)	1220±150	430±50	0.35±0.06	0.03
WR 124	WN8 (SB1)	740 ±5	250±5	0.34±0.01	0.10
WR 156	WN8	650 ±10	230±5	0.35±0.01	0.04
WR 108	WN9	1140±60	120±50	0.10±0.04	–
Brey 91	Ofpe/WN9	500 ±50	120±50	0.24±0.10	–
Be 381	Ofpe/WN9	375 ±40	80±50	0.21±0.13	–
R 84	WN9	400 ±40	110±50	0.28±0.13	–
Sk -6640	Ofpe/WN9-10	300 ±30	20±25	0.07±0.09	–

[a] derived via model fitting (Schmutz 1997) of the He II emission profiles in the UV region.
[b] estimated by Antokhin et al. (1997) as a by-product of the light curve solution.
[c] our estimation of v_∞.

we have to reject $T_\star$. The stellar temperature decreases more or less monotonically as the spectral subtype goes from WN3 to WN8 (Hamann & Koesterke 1998), which is inconsistent with the non-monotonic v_{phot}/v_∞ vs. spectral subtype behavior. Collecting data from Crowther et al. (1995 a-d) and Hamann & Koesterke (1998), we find no correlation between $L_\star$ and v_{phot}/v_∞ (Fig. 3). On the other hand, there is a clear $\dot{M} \leftrightarrow v_{phot}/v_\infty$ dependence, with a steep rise of $\dot{M}$ for $v_{phot}/v_\infty \geq 0.35$ (Fig. 3). Naturally, the latter dependence is transformed into 'threshold'-like behavior in plots of $\dot{M}v_\infty/L/c$ ('wind efficiency') vs. v_{phot}/v_∞, or $\dot{M}/(4\pi v_\infty R_\star^2)$ ('wind density') vs. v_{phot}/v_∞ (not shown). Another interesting trend can be revealed by comparing with stellar variability (Fig. 3). For this we calculate the $\sigma^2_{obs}/\sigma^2_{instr}$ ratio (Fisher statistics) from the HIPPARCOS photometric data sets (Marchenko et al. 1998b) and apply 99% detectability threshold, where σ_{obs} corresponds to the directly observed scatter, and σ_{instr} is deduced from the magnitude-dependent instrumental detectability limit. We immediately notice that practically all stars with significant variability tend to have $v_{phot}/v_\infty > 0.3$. Additionally, there is no notable dependence of $\sigma^2_{obs}/\sigma^2_{instr}$ on $L_\star$ or $\dot{M}$ to interfere with the suggested $\sigma^2_{obs}/\sigma^2_{instr} \leftrightarrow v_{phot}/v_\infty$ dependence. Far more data need to be collected before one can relate this intriguing trend to any pulsationally-supported mass loss phenomenon.

3.2. v_{phot}/v_∞ *ratios derived from profile fitting*

How close are our empirical evaluations to the real values of v_{phot}/v_∞? At least some indication can be provided by profile fitting with the SEI method (Sobolev method with exact integration: Lamers et al. 1987). An iterative fitting of the observed line profiles (13 stars in total in the optical, from our own data) is performed with the parameterized velocity and optical depth laws (see Lamers et al. 1987 for more details, including the justification of the chosen optical depth law):

$$v(x) \;=\; \frac{v_{phot}}{v_\infty} + (1 - \frac{v_{phot}}{v_\infty})(1 - \frac{1}{x})^\beta \;,$$

Table 2. Parameters used in the SEI profile fitting

Star	line	τ_{tot}	β	α_1	α_2	ε_0	B_0	a_T	v_{turb}/v_∞
WR 6	NV 4603,4619	0.0035	3.0	4.0	6.7	1.8	1.0	0.20	0.30
	He II 4686	1.1	–	4.0	0.30	9.9	–	–	–
WR 139	NV 4603,4619	0.055	1.2	0.90	2.4	4.3	1.0	0.20	0.10
	He II 4686	1.9	–	2.2	1.0	7.0	–	–	–
WR 151	NV 4603,4619	0.035	1.1	0.90	4.3	5.0	1.2	0.50	0.05
	He II 4686	0.80	–	1.3	3.7	50.0	–	–	–
WR 134	NV 4603,4619	0.12	3.0	0.30	4.0	1.2	1.2	0.20	0.16
	He II 4686	0.90	–	5.0	0.2	5.4	–	–	–
WR 136	NV 4603,4619	0.14	2.0	0.50	2.1	0.73	1.1	0.30	0.11
	He II 4686	0.67	–	2.2	0.45	19.0	–	–	–
WR 138	NV 4603,4619	0.25	0.60	0.30	3.0	5.5	1.0	0.20	0.20
	He II 5412	0.23	–	3.5	3.0	22.0	–	–	–
WR 141	NV 4603,4619	0.032	2.9	1.2	3.5	0.90	1.2	0.30	0.17
	He II 4686	0.59	–	1.8	0.20	8.0	–	–	–
WR 155	NV 4603,4619	0.025	1.9	0.50	5.0	0.01	1.2	0.0	0.12
WR 148	He I 4471	0.018	2.0	0.90	3.5	7.0	1.0	0.20	0.25
WR 40	He II 5412	0.20	1.2	0.7	2.5	20.0	1.0	0.70	0.20
	He I 5876	0.82	–	2.5	1.1	29.0	–	–	–
WR 123	He II 5412	0.49	0.65	0.40	3.9	21.0	1.2	0.90	0.18
	He I 4471	0.42	–	3.3	2.5	5.5	–	–	–
WR 124	He II 5412	0.20	1.4	1.4	1.7	2.7	1.1	0.90	0.35
	He I 4471	0.69	–	3.5	0.50	2.8	–	–	–
WR 156	He II 5412	0.075	2.5	1.8	2.0	5.4	1.0	1.0	0.20
	He I 4471	0.30	–	2.7	1.3	3.0	–	–	–

$$\tau(v) \;=\; \tau_0(\frac{v_{phot}}{v_\infty})^{\alpha_1}[1-(\frac{1}{x})^{\frac{1}{\beta}}]^{\alpha_2}\;,$$

with $x \equiv r/R_\star$, and $\beta, v_{phot}, \tau_0, \alpha_1, \alpha_2$ taken as free parameters. The code explicitly allows for local turbulence in the wind, with parameter v_{turb}. The remaining 3 parameters are related to the source function: ε_0 controls the collisional term in the source function; B_0 provides the Planck function in the wind, normalized to the continuum; a_T is the coefficient controlling the temperature distribution in the wind, so that $a_T > 0$ signifies an outwardly decreasing temperature. In Table 2 we list the values of the parameters providing the best match with the observed profiles (cf. Fig. 1) for the 13 stars for which we have high-quality digital data. The known values of v_∞ are taken from Table 1. We do not intend to use v_∞ as an independent parameter. Since this is the only parameter which can be directly derived from observations with relatively high accuracy ($\sim 10\%$), we prefer to keep it fixed. When using v_∞ as a free parameter in our simulations, we are able to restrict it only loosely, within $\pm 30\%$, owing to the large number of variables. This accuracy is typical for the rest of the parameters as well.

Whenever possible, we start with the NV 4603, 4619 Å doublet, then proceed to the He I, He II lines with all but 3 model parameters fixed as for the optimal NV fit. These 3 parameters ($\tau_0, \alpha_1, \alpha_2$) are responsible for the radial distribution of the optical depth and, naturally, may vary from line to line. As soon as we find an appropriate model for the He I and/or He II profiles (which may incorporate some change of the values adopted for the best NV fit), we return to fitting of the NV lines. The procedure usually converges after 2-3 iterations. During the fitting we convolve the modeled line with the instrumental profile (3-pixel Gaussian) and allow for the presence of a companion in the binary systems (using the known or assumed luminosity ratios for WR 138, 139, 141, 148, 151, 155). We provide model estimations of $\mathrm{v_{phot}/v_\infty}$ in Table 1 and we plot the derived $\mathrm{v_{phot}/v_\infty}$ theoretical limit along with the data in Fig. 2, averaging all calculated values within one spectral subclass. We stress that this limit should be treated only as indicative, due to the factor-of-two uncertainty arising from the parameterization of the wind velocity law and radial dependence of the line optical depth. The achieved accuracy in $\mathrm{v_{phot}}$ is $\sim 50\%$ for $\mathrm{v_{phot}/v_\infty} < 0.1$ and $\sim 30\%$ for $\mathrm{v_{phot}/v_\infty} > 0.1$.

There is one interesting trend emerging from the simulations. We find the highest discrepancies between the observed and modelled $\mathrm{v_{phot}/v_\infty}$ ratios for some WN5-6 stars (WR6 and WR134 in particular) and *all* WN8 stars. As we already mentioned, WN8 stars are unusually active and subject to large-scale line profile variations, especially affecting the P Cygni absorptions (Marchenko et al. 1998a). The same is true for WR6 (Morel et al. 1997) and, to a lesser extent, WR134 (Morel et al. 1998). These variations may call for increased values of v_{turb} in the SEI simulations. Indeed, we find $v_{turb} = (0.27 \pm 0.03)v_\infty$ for WR6, WR134 and WNL stars, and $v_{turb} = (0.14 \pm 0.02)v_\infty$ for the rest of our sample. This may serve as an indication that the empirically derived v_{phot} could be seriously biased by the variability induced by large-scale structures in the winds of WR6, WR134 and WN8 stars.

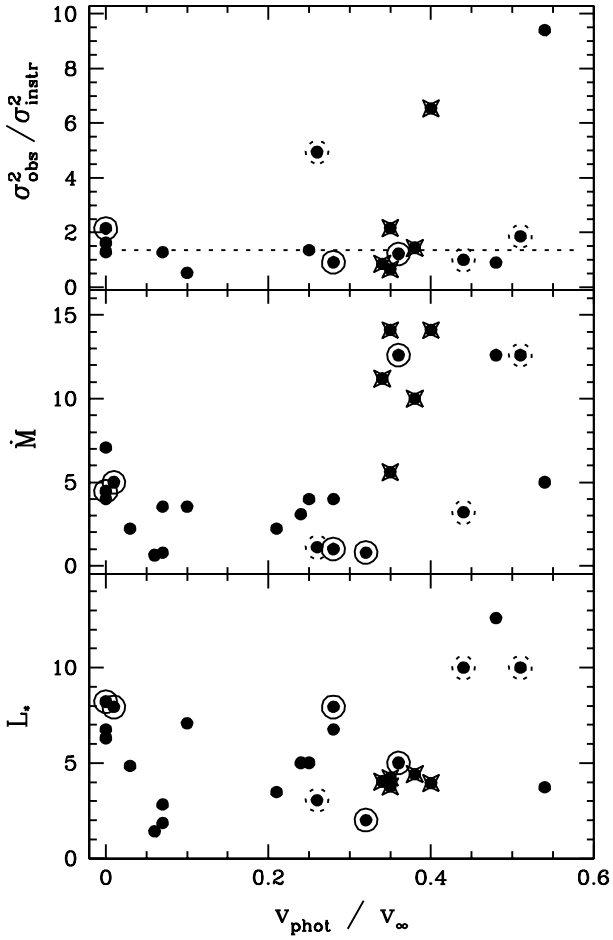

Fig. 3. The relationships between v_{phot}/v_∞ and: *upper panel* the stellar variability factor (see text for more details), where the dashed line corresponds to 99% detectability limit; *middle panel* the mass loss rate, in $10^{-5} M_\odot/yr$ units; *bottom panel* stellar luminosity, $10^5 L_\odot$ units. The full-line encircled points correspond to close WR+O binaries; dash-line encircled points denote suspected WR+c binaries; starred symbols mark WN8 stars.

4. Conclusions

We conclude that no less than 50% (in some cases up to 100%) of the wind's terminal velocity is gained in the optically thin part of the WR wind. This lessens the requirements of a subphotospheric velocity boost, and, on the other hand, signifies the importance of the ionization stratification in the optically thin part of the WR wind (Schulte-Ladbeck, Eenens & Davis 1995) which enhances the exerted radiative force via effectively increasing the overlap of the wind-driving spectral lines (cf. Lucy & Abbott 1993; Springmann 1994; Gayley et al. 1995; Schmutz 1997). Both WN7 and WN8 stars may deviate in the physical characteristics of their winds (wind velocity gradient in WN7 stars, and unusually high wind 'turbulence' in WN8 stars) from the rest of the WN population.

Acknowledgements. We thank our referee, W. Schmutz, for detailed and well argumented criticisms, helping us to clarify some important details, and paricularly for the suggestion to look for any dependence of v_{phot}/v_∞ on fundamental stellar parameters.

References

Abbott, D.C., Conti, P.S. 1987, ARA&A 25, 113
Antokhin, I. I., Cherepashchuk, A. M., Yagola, A.G. 1997, ApSS 254, 111
Crowther, P.A., Hillier, D.J., Smith, L.J. 1995a, A&A 293, 172
Crowther, P.A., Hillier, D.J., Smith, L.J. 1995b, A&A 293, 403
Crowther, P.A., Smith, L.J., Hillier, D.J. 1995d, A&A 302, 457
Crowther, P.A., Smith, L.J., Hillier, D.J., Schmutz, W. 1995c, A&A 293, 427
Eichler, D., Bar Shalom, A., Oreg, J. 1995, ApJ 448, 858
Gayley, K.G., Qwocki, S.P., Cranmer, S.R. 1995, ApJ 442, 296
Hamann, W.-R., Koesterke, L. 1998, A&A, in press
Hillier, D.J. 1991, A&A 247, 455
Lamers, H.J.G.L.M., Cerruti-Sola, M., Perinotto, M. 1987, ApJ 314, 726
Lucy, L. B., Abbott, D. C. 1993, ApJ 405, 738
Marchenko, S.V., Moffat, A.F.J., Eenens, P.R.J., Cardona, O., Echevarria, J., Hervieux, Y. 1997, ApJ 485, 826
Marchenko, S.V., Moffat, A.F.J., Eversberg, T., Hill, G., Tovmassian, G., Morel, T., Seggewiss, W. 1998a, MNRAS 294, 642
Marchenko, S.V., Moffat, A.F.J., van der Hucht, K.A., et al. 1998b, A&A 331, 1022
Moffat, A.F.J., Marchenko, S.V., Seggewiss, W., et al. 1998, A&A 331, 949
Moffat, A.F.J., Seggewiss, W. 1978, A&A 70, 69
Morel, T., St-Louis, N., Marchenko, S. 1997, ApJ 482, 470
Morel, T., Marchenko, S., Eenens, P., et al. 1998, ApJ, submitted
Niemela, V.S., Cabanne, M.L., Bassino, P.L. 1995, Rev. Mex. A&A 31, 45
Rochowicz, K., Niedzielski, A. 1995, Acta Astron. 45, 307
Schmutz, W. 1997, A&A 321, 268
Schulte-Ladbeck, R.E., Eenens, P.R.J., Davis, K. 1995, ApJ 454, 917
Springmann, U. 1994, A&A 289, 505
St-Louis, N. 1990, PhD Thesis, University College, London
St-Louis, N., Dalton, M., Marchenko, S.V., Moffat, A.F.J., Willis, A.J. 1995, ApJL 452, L57
van der Hucht, K.A., Hidayat, B., Admiranto, A.G., Supelli, K.R., Doom, C. 1988, A&A 199, 217
Willis, A. J. 1982, MNRAS 198, 897
Willis, A. J., & Stickland, D. J. 1990, A&A 232, 89